Atomic Force Microscopy of Gel-Drawn Ultrahigh Molecular Weight Polyethylene

S. N. Magonov,† S. S. Sheiko,‡ R. A. C. Deblieck,§ and M. Möller*,†

Faculteit der Chemische Technologie, Universiteit Twente, P.O. Box 217, 7500 AE Enschede, The Netherlands, Freiburger Materialforschungs-Zentrum, Albert-Ludwigs-Universität, Stefan-Meier-Strasse 31A, D-7800 Freiburg, Germany, and DSM Research, P.O. Box 18, 6160 MD Geleen, The Netherlands

Received August 5, 1992; Revised Manuscript Received November 12, 1992

ABSTRACT: Gel-drawn ultrahigh molecular weight polyethylene was studied by atomic force microscopy (AFM). Three-dimensional surface profiles were recorded for tapes drawn to different extents. AFM images allowed the discrimination of different well-defined levels of the fibrillar morphology: (i) bundles of microfibrils with a diameter between 4 and 7 μm strongly depending on the elongation; (ii) microfibrils with a diameter between 0.2 and 1.2 μm which also decreased with increasing draw ratio; (iii) nanofibrils which form the elementary fibrillar building blocks; and (iv) regular chain patterns on the molecular level which correspond to the crystalline packing of polyethylene chains at the surface of the nanofibrils. The nanofibrils were formed during the initial conversion of lamellae to fibrillar crystallites and did not change considerably in diameter up to draw ratios of $\lambda = 70$.

Introduction

Fibers with properties which approach the theoretical limits in strength and modulus can be obtained by principally different technologies. These are spinning lyotropic liquid crystalline solutions of "stiff rod" polymers, e.g., polyaramides,[1,2] and the so-called gel-spinning technology which was developed for flexible polymers like linear polyethylene.[3,4] Nearly perfect uniaxial orientation of the macromolecules represents the basic requirement for the preparation of strong polymer fibers, and the high-performance properties depend strongly on structural defects within the drawn material. In the case of the gel-spinning technique, the polymer is crystallized from dilute or semidilute solution and thus brought into a state where solid-state processing to ultrahigh draw ratios is possible. In a complicated process, the original chain-folded lamella structure is transformed into a chain-extended fibrillar morphology. Not only the deformation process but also the resulting fiber structure has been the subject of many recent studies.[5–8] The most widely accepted model for the solid-state deformation of polyethylene has been proposed by Peterlin[9] and was recently discussed in detail by van Aerle and Braam as a three-stage process for the interpretation of X-ray studies on the deformation of gel-crystallized ultrahigh molecular weight polyethylene (UHMW-PE).[10,11] However, still it was not possible to obtain an answer on all questions regarding the transformation of lamellae into microfibrils, the details of the fibrous structure, and the elementary unit of the fibrillar morphology.

So far, our knowledge is mainly based on studies by spectroscopic and diffraction methods. Direct visualization of the fiber structure was possible by scanning (SEM) and transmission (TEM) electron microscopy. While SEM is limited in resolution, TEM requires sophisticated sample preparation involving either ultramicrotomy and staining or fracturing, etching, and replication where the latter severely limits the structural details present in the image. Recently, substantial progress was achieved in minimal-dose high-resolution electron microscopy of crystalline polymers, and a corresponding study on ultradrawn gel films of UHMW-PE[12] allowed the identification of the modification of separate crystalline blocks yielding a rather detailed description of their mutual arrangement.

An alternative and complementary imaging tool, also for polymer materials, became available when the atomic force microscopy (AFM) was developed. This scanning probe technique is based on the detection of force profiles between individual atoms of a probing needle and the investigated surface.[13] The unique feature of the method is its capability to monitor a surface in real time/space within the range from hundreds of microns to angstroms. AFM can be applied almost to all kinds of materials because of the universal character of the employed interaction, and it has already been used successfully for studies on several crystalline and semicrystalline polymer materials.[14–18] For solid-state extruded polyethylene and poly(tetrafluoroethylene), it was shown that it is possible to image individual chains. Also monocrystals, solvent-cast films, compact fibers, and surfaces prepared by microtomy are suitable for AFM analysis. Limitations result from the required rigidity of the studied material and the minimum tip radius (ca. 40 nm) of the pyramidal probe.

This work reports first AFM studies on gel-drawn UHMW-PE. As will be described below, AFM can reveal morphological details which are at the limit of or even beyond possibilities of conventional electron microscopy and thus help to document the structural changes which occur during the drawing process and which control the properties of the final product.

Experimental Section

Materials. Polymer gels were prepared from a 1.5% by weight solution of UHMW-PE (Hizex 240M, $M_w = 1.5 \times 10^6$) in *p*-xylene as described by Smith et al.[19] The solution was stirred at 130 °C under nitrogen until the Weissenberg effect developed and afterward kept for 2 h at 130 °C. The solution was cast to a gel film of about 0.5-cm thickness, and the gel was dried for several days at ambient conditions. Semitransparent films of ca. 50-μm thickness were obtained. The film was cut in tapes (20 mm in length, 3 mm in width), which were drawn at 125 °C to draw ratios of $\lambda = 10$, 25, and 70.

In order to allow observation of the bulk morphology of fibers at the highest draw ratio, the PE fibers were stretched over a polystyrene tile ($10 \times 10 \times 1.6$ mm^3) and glued by means of a

* To whom correspondence should be sent.
† Albert-Ludwigs-Universität.
‡ Universiteit Twente.
§ DSM Research.

0024-9297/93/2226-1380$04.00/0

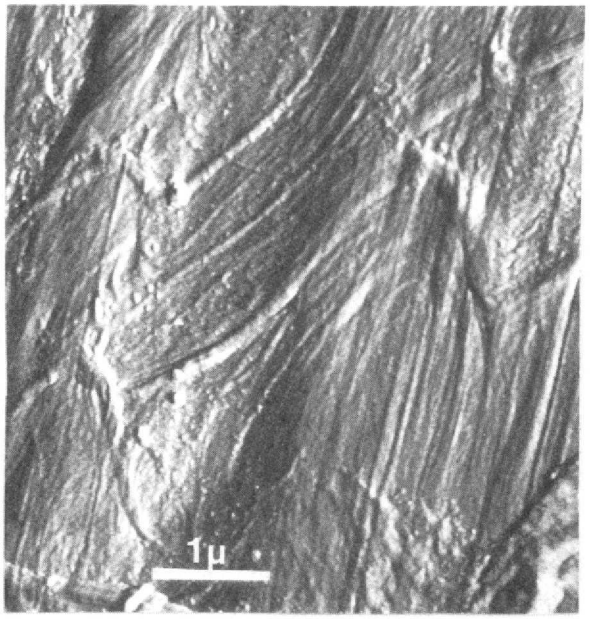

Figure 1. Low-magnification force imaging mode AFM micrograph of the surface of a cryomilled ultradrawn PE sample (λ = 100).

polystyrene/THF solution. After drying, the fibers are sufficiently fixed to allow for cryomilling in a Reichert–Jung ultracut E at a specimen temperature of −150 °C, a milling frequency of 3000 rpm, and an advancing speed of 1.5 mm/s. Progress of the milling process was monitored under a reflected light microscope, so as to observe whether the fibers have been cut open. The cutting depth of the final path was 1 μm. Although, despite the cooling, such a procedure is bound to cause a certain amount of fibrillation, there were a lot of areas formed where the underlying fibrillar morphology remained untouched, as can be seen in the low-magnification AFM micrograph in Figure 1.

AFM. Atomic force scanning micrographs were recorded with a Nanoscope II (Digital Instruments, Inc., Santa Barbara, CA) at ambient conditions. Depending on the desired resolution, different piezoelements were used for the examination of smaller or larger areas, i.e., 1 × 1 and 16 × 16 μm^2, respectively. A V-shaped cantilever of 200 μm in length with a Si_3N_4 tip (spring constant 0.12 N/m) was used to probe the surface (NanoProbes, Digital Instruments, Inc.). Imaging of the PE surface were recorded in two different modes. Three-dimensional surface profiles were obtained in the height (constant force) mode. In this case, the voltage is measured which is applied to the piezoelement in order to keep the probing force (z-direction) constant. Complementary measurements were made in some cases in the force imaging mode (quasi constant height regime), which allows us to image the morphological details with a better contrast. In this case, the feedback is not effective and deflections of the cantilever with the probing tip are registered and are proportional to the acting force. The tapes were aligned approximately along the y-axis of the microscope head and measurements were always reproduced in several places on each tape. In special cases, atomic-scale AFM images were low-pass filtered. In some cases, rotation of the sample around the surface normal helped to improve the image quality.

SEM. Scanning electron micrographs were obtained using a Hitachi S-800 scanning electron microscope operated at low voltage (<6 keV). Films of the dried PE gel were slightly coated with carbon or investigated without any coating.

Results and Discussion

Gel-crystallized polyethylene was prepared by cooling a semidilute solution of ultrahigh molecular weight polyethylene to ambient temperature. When the solvent was removed, a mat of interconnected PE lamellar crystallites was obtained which could be drawn to tapes at temperatures above the α-transition. From X-ray[19] and electron diffraction,[20] it is known that all lamellae are oriented parallel with the film surface.

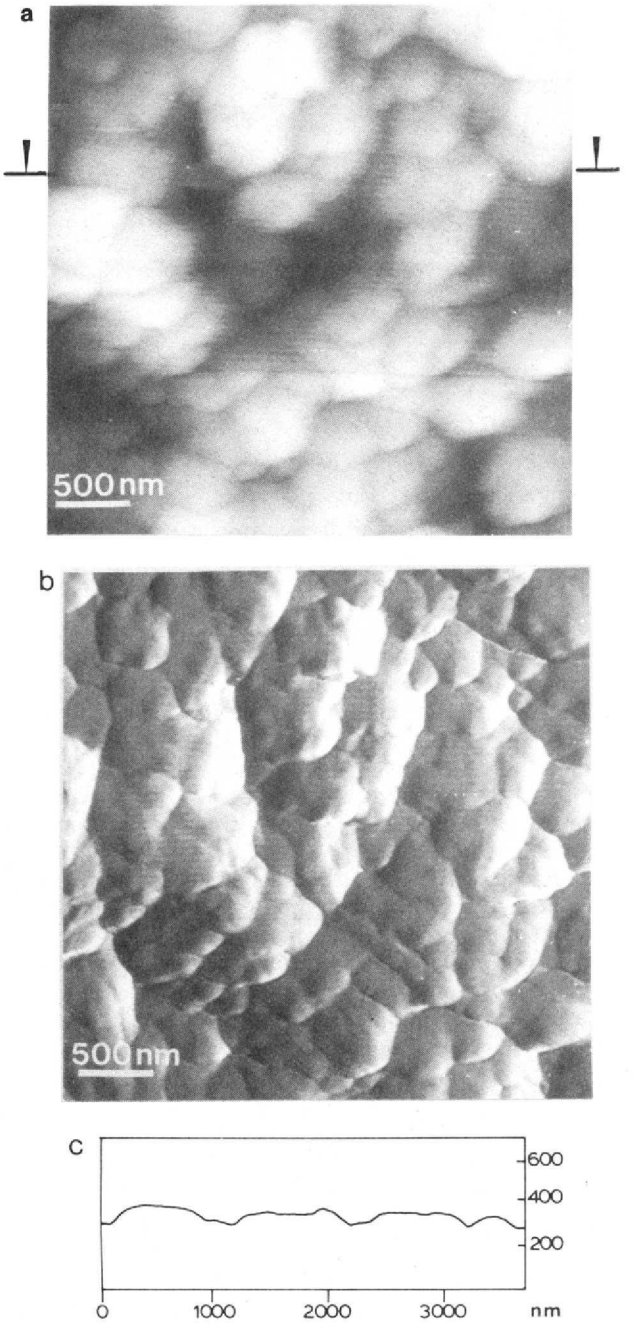

Figure 2. Surface of a dried, gel-crystallized polyethylene film: (a) micrograph recorded in the height mode; (b) micrograph recorded in the force mode; (c) surface profile.

Parts a and b of Figure 2 show surface images of the film obtained from the gel after removal of the solvent but before drawing. Small, convex grains with diameters in the range of 100–400 nm were observed to be characteristic for the surface of the gel. The grain pattern can be seen more clearly in Figure 2b which had been recorded in the force mode. As shown by comparison of parts a and b of Figure 2, the higher contrast of a force profile map can be useful for the visualization of morphological details. Figure 2c shows a profile along the line indicated in Figure 2a demonstrating average variations in the height around 100 nm.

However, AFM experiments in different areas of the film indicated a considerable roughness of the gel surface. In some areas it was not possible to record surface profiles because the roughness exceeded the AFM depth of field

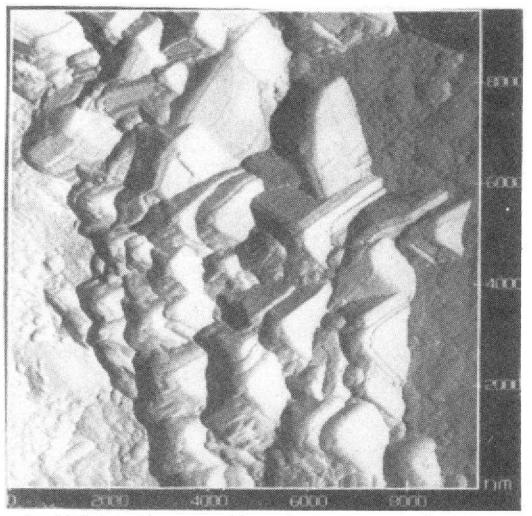

Figure 3. AFM tip image artifacts in a micrograph of the surface of a dried, gel-crystallized polyethylene film recorded in the force mode.

(<4 μm) or the images were severely distorted by surface roughness related artifacts (Figure 3). These "tip image" artifacts result when steep elevations in the surface are of similar size or even smaller width than the probing peak of the tip.[21,22] Such protrusions actually probe the surface of the tip and write its image into the AFM micrograph. Usually, the tip images can be recognized by their sharp demarcation and the multiple occurence of the same pyramidal structure.

In order to verify the surface topology shown in Figure 2, scanning electron microscopy experiments have been performed. Figure 4a represents an SEM overview of the surface morphology of a solution-crystallized film. Flat areas are surrounded or cut by corrugations with height variations up to 5 μm. It is obvious that AFM pictures like those in Figure 2 could only be obtained from the flat areas. Comparison of the SEM micrograph in Figure 4b with the AFM image in Figure 2b demonstrates that both techniques give similar results for the surface morphology in the flat areas. Convex grains of diameters between 100 and 200 nm (in the AFM micrograph up to 400 nm) form the basic element of the surface morphology.

Because of the parallel arrangement of the PE lamella crystals with respect to the film surface known from the literature,[19,20] the grains can be assigned to stacked polyethylene lamellae crystals. Protrusions may result from lamellar edges of crystals which were not deposited parallel to the film surface.

Upon drawing, the most significant morphological changes occur in a narrow necking region which separates the original lamellar material from the drawn fibrous sample. Until all material is transformed through the necking area, only the size of the neck increases on the expenses of the little deformed lamellar material while the draw ratio remains rather constant. During this stage the fibrils within the neck are not perfectly oriented and appear also to contain remnants of the original lamellae.[10,11] Further drawing of the neck leads to an improvement of the fibrillar organization. In the case of the tapes reported here, the necking resulted typically in an initial draw ratio λ = 8–10, while the deformation outside the neck was less than 30%.

The structure within the neck can be monitored by AFM at different draw ratios of the PE tapes. Figure 5a shows the surface of a PE tape with a draw ratio of λ = 10 as obtained directly after necking. Bundles of microfibrils are depicted. The bundles are not very well-defined, and their average diameter varies largely between 4 and 7 μm depending on the location where the image has been recorded. However, the surface profile shows that the corrugations are locally regular. The constituent microfibrils are more homogeneous in thickness, having a diameter between 0.5 and 1.2 μm. Although the structure

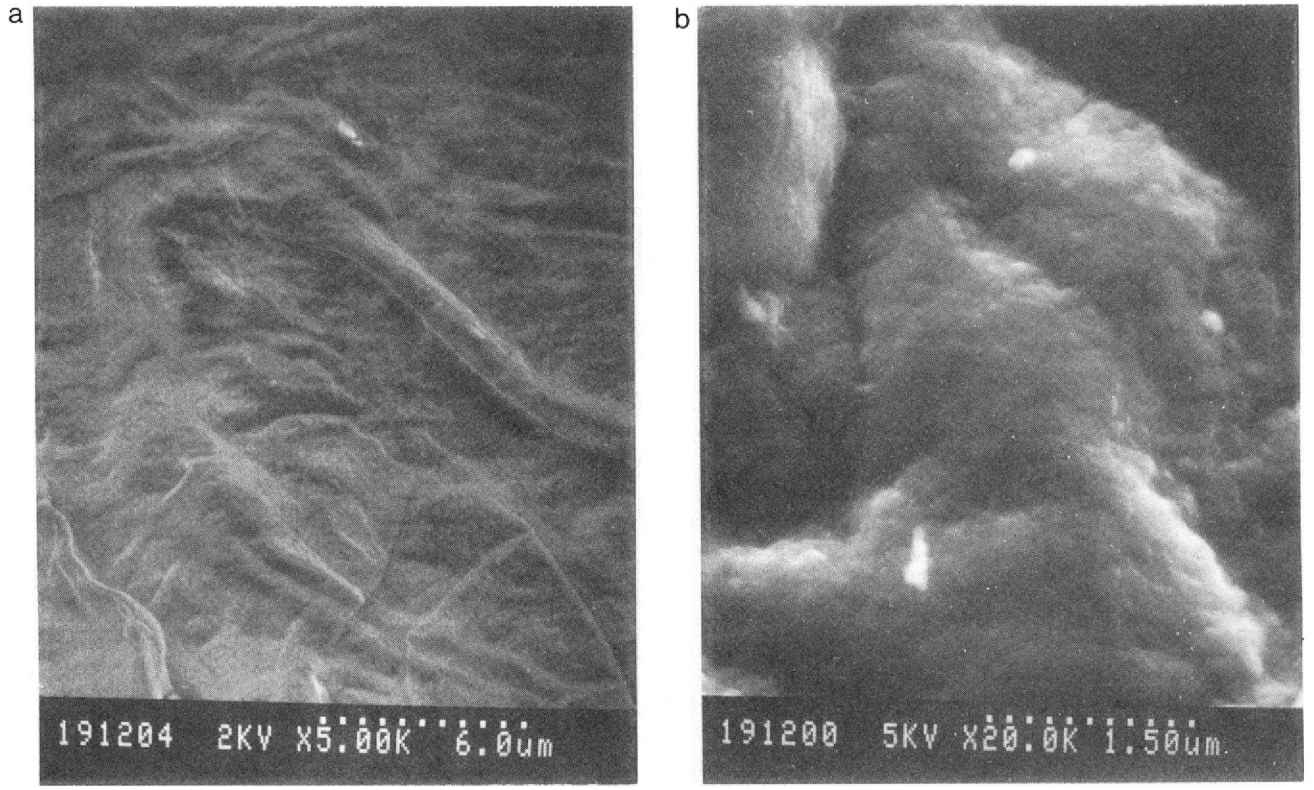

Figure 4. Scanning electron micrographs of the surface of a dried, gel-crystallized polyethylene film. The sample was coated with a thin carbon film: (a) overview; (b) same magnification as the image in Figure 2b.

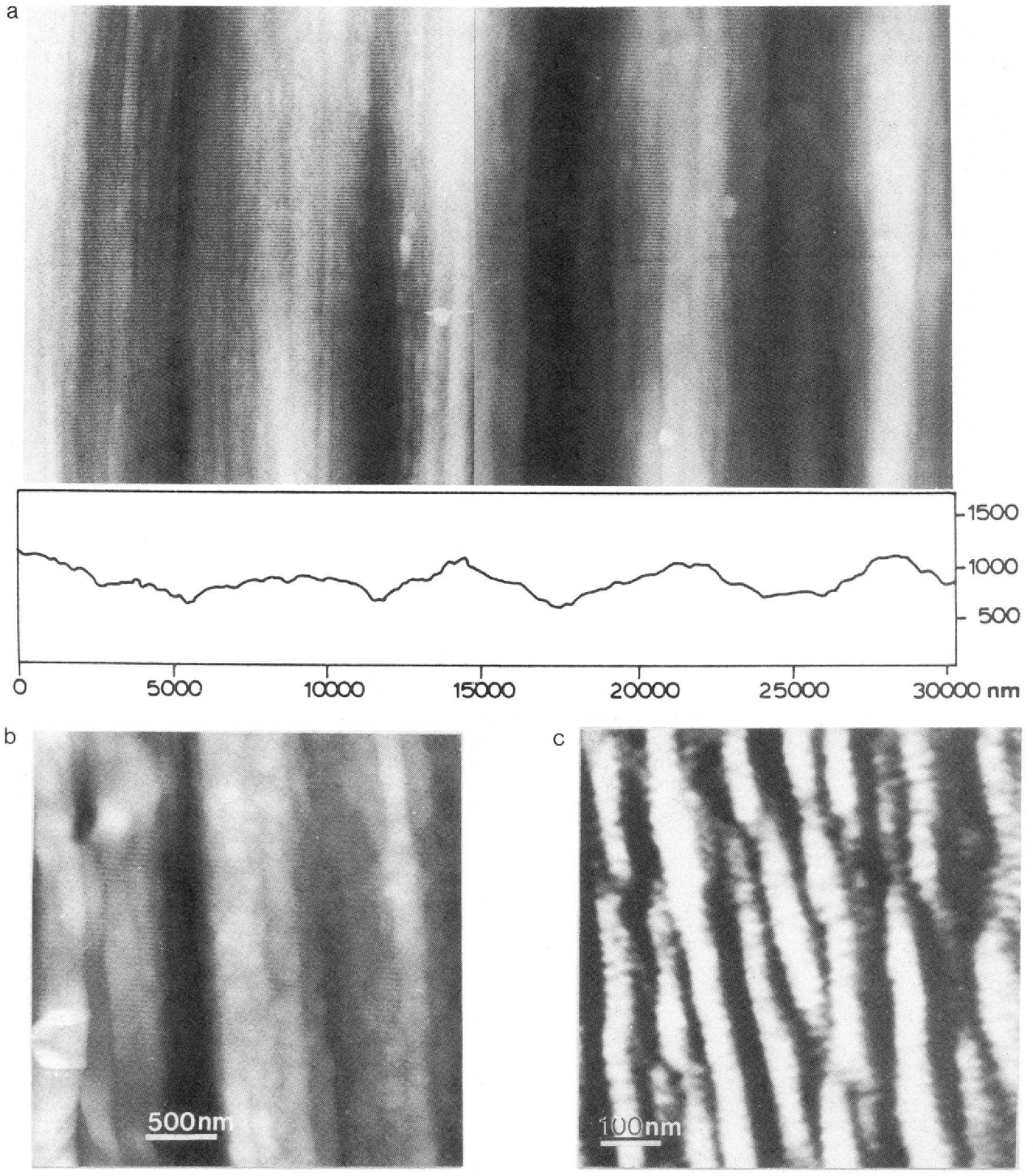

Figure 5. Surface images from the neck of gel-drawn PE with a draw ratio of $\lambda = 10$: (a) 30×15 μm^2 section with a horizontal surface profile showing bundles of microfibrils; (b) 3.3×3.3 μm^2 enlargement showing corrugations of the microfibrils which might be caused by remnants of the original lamellae; (c) 0.8×0.8 μm^2 section showing an area where nanofibrils have been formed.

appears to be rather homogeneous on the micrometer scale, the enlargements in parts b and c of Figure 5 demonstrate the heterogeneous nature of the deformation process. In Figure 5b, one can recognize not only the microfibrillar structure but also blocklike patterns (ca. 100 nm in diameter). The latter may be assigned to remnants of the lamellae. In contrast, Figure 5c shows the structure of another microfibril which itself is formed from a bundle of even smaller fibrils with diameters of about 40–80 nm. Apparently, these small "nanofibrils" form the building blocks of all microfibrils. Branching and interweaving of nanofibrils can be seen clearly in Figure 5c. Obviously, Figure 5b represents the fine structure of an early stage of the transformation from lamellae to fibrils where the lamellae are not yet completely transformed.

In a first summary, the AFM images discriminated three well-defined levels of the fibrillar morphology: (i) bundles of microfibrils, (ii) microfibrils, and (iii) nanofibrils. While bundling of microfibrils to fibrils is well described,[23] it is a controversial observation that microfibrils are constructed from apparently well-defined smaller nanofibrils which represent the constituent thread of the microfibrils.

Surface images of tapes which had been drawn to higher draw ratios, i.e., $\lambda = 25$ and 70, are compared in Figure 6. Again, the micrographs have been recorded in the height mode as well as in the force mode. The microfibrils

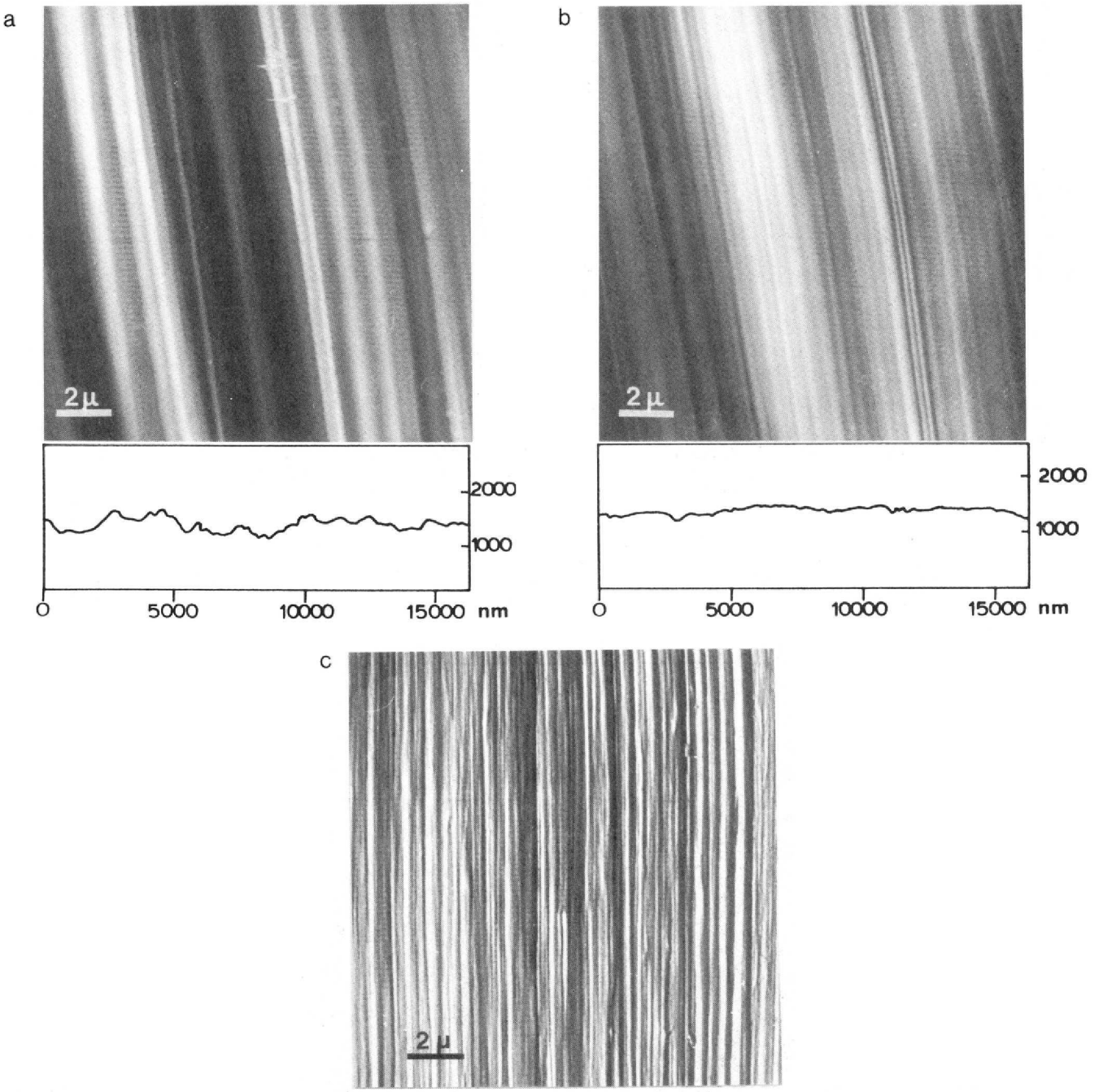

Figure 6. 16 × 16 μm^2 atomic force micrographs of polyethylene tapes drawn to different elongations: (a) $\lambda = 25$, height mode image; (b) $\lambda = 70$, height mode image; (c) $\lambda = 70$, force mode image. Surface profiles are given below the height mode images.

represent the main structural feature of the images. An improvement of the microfibril orientation and a decrease in their width becomes evident as the draw ratio increases, while defects like twisting and interlacements are removed. Profiles of the tape surface demonstrate that the corrugation became smaller at higher draw ratios, resulting in a smoother surface of the tapes and indicating that the bundling of microfibrils is less pronounced at higher elongations.

Figure 7 gives a corresponding comparison of micrographs which have been observed when smaller areas were scanned at high resolution. Within the limits of draw ratios between $\lambda = 10$ and 70, the microfibrils were always found to be formed from smaller strings of diameters between 20 and 90 nm (mainly about 40–60 nm). Thus, it is a peculiar observation that the smallest fibrillar elements, i.e., the nanofibrils, were formed in the initial deformation steps during necking and did not change their width significantly when the tapes were drawn further.

The question has to be raised whether the observation of nanofibrils as a fundamental fibrillar element can be regarded to be representative for the bulk material, although it has been observed only at tape surfaces so far. To that end, AFM images were also recorded from surfaces of PE tapes that had been cut open by means of cryomilling as described in the Experimental Section. These tape surfaces can be regarded to be representative of the bulk morphology *d*. Figure 7c shows an AFM micrograph obtained from such a surface. It reveals the same nanofibrillar morphology that was already demonstrated in the micrographs acquired from the tape surfaces, i.e., Figures 5c and 7a,b.

Observations at a higher magnification allow visualization of the molecular surface structure of the nanofibrils. Figure 8 shows a highly magnified height mode micrograph of the surface of a nanofibril in a tape drawn to $\lambda = 70$.

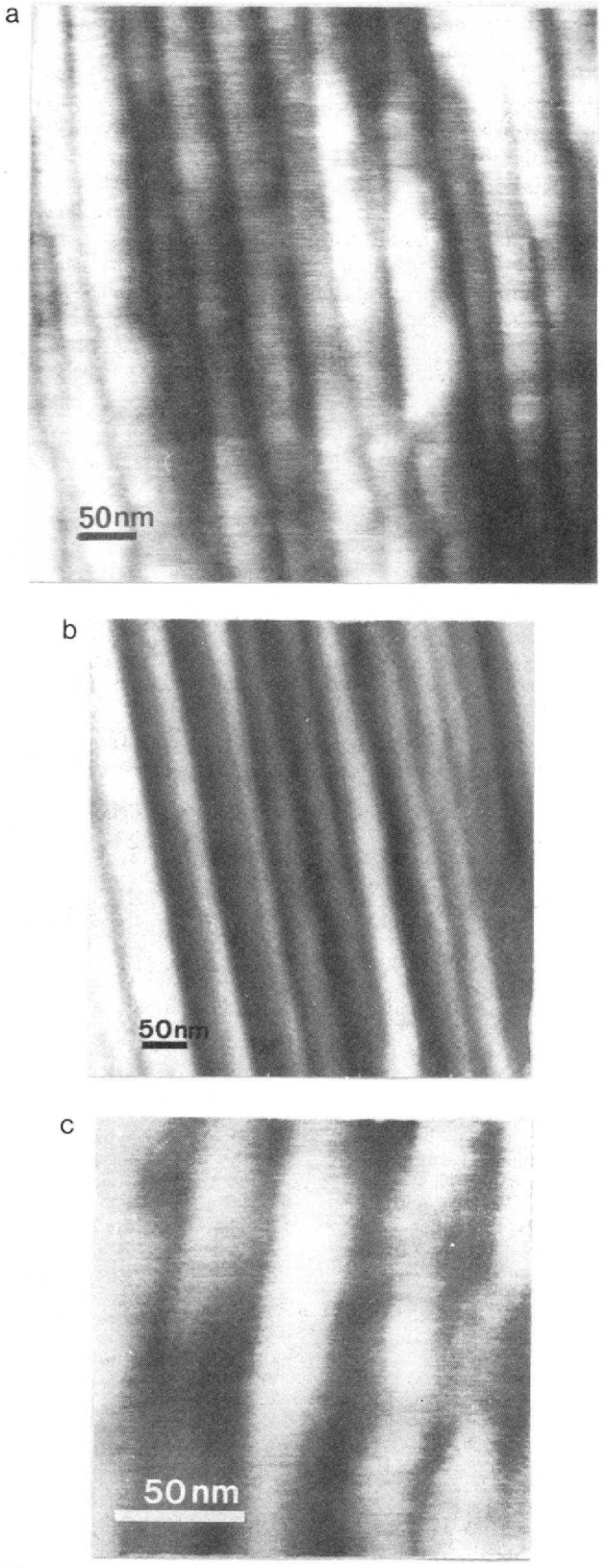

Figure 7. Enlarged sections showing the nanofibrillar substructure of the microfibrils: (a) $\lambda = 25$, height mode image; (b) $\lambda = 70$, height mode image; (c) image of the surface of a cryomilled sample, $\lambda = 100$.

Remarkably clear, the image features regularly aligned strings which are packed with a period of about 5 Å. It appears obvious that Figure 8 represents the regular arrangement of polyethylene chains at the surface of the nanofibrils. As no intermediate texture could be recognized and in regards to the rather uniform diameter of the

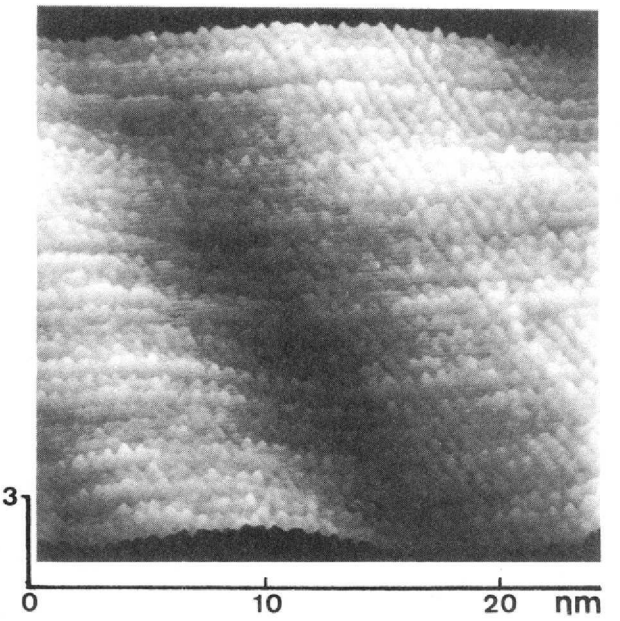

Figure 8. Three-dimensional low-pass-filtered representation of two nanofibrils showing parallel strings representing individual polyethylene chains, $\lambda = 70$.

nanofibrils, it can be concluded that the observed nanofibrils represent an elementary building block unit of the fibrillar structure in gel-drawn UHMW-PE.

The molecular resolution allows comparison of the packing of the chains in the surface with the X-ray results on the bulk structure.[10,11,24] A period between 4.8 and 5.2 Å was measured in Figure 8 which corresponds with the d_{010} interchain distance of orthorhombic polyethylene. The corresponding orientation of the crystal planes is in good agreement with the result of a biaxial orientation process, as has been shown by IR dichroism[25] and X-ray diffraction experiments.[10,24] Upon uniaxial elongation of gel-crystallized UHMW-PE tapes, the *b*-axis of the unit cell tends to align preferentially parallel with the tape surface. This orientation becomes more pronounced with increasing draw ratio. Consequently, different distances were found at small draw ratios which correspond to both the *b*- and *a*-axes modulated by the tilt angle of the investigated surface (at an elongation of $\lambda = 10$, the AFM interchain distance varied from 4.8 to 8.3 Å). At higher draw ratios, the 010 periodicity becomes dominant.

Finally, Figure 9 demonstrates that, in stable imaging conditions, atomic force microscopy has the potential to resolve the chain structure of the all-trans planar PE. The image in Figure 9a shows a somewhat distorted though not irregular pattern of elevations along the chains. From the surface profile along the chain and from the corresponding optical transform in Figure 9b an average period of 2.5 Å is measured, which corresponds well with the 001 repeat distances along the chain axis.

Conclusions

AFM images can visualize yet not observed details of the surface structure. Although deviations form the bulk structure have to be considered, a rather distinctive picture emerges. AFM shows the formation of nanofibrils as elementary building units of ultradrawn PE tapes. Their dimensions and the way they are assembled may represent crucial arguments for the explanation of the deformation mechanism and modeling of the mechanical properties of ultradrawn polyethylene fibers. AFM clearly indicates the heterogeneity of the deformation process at the

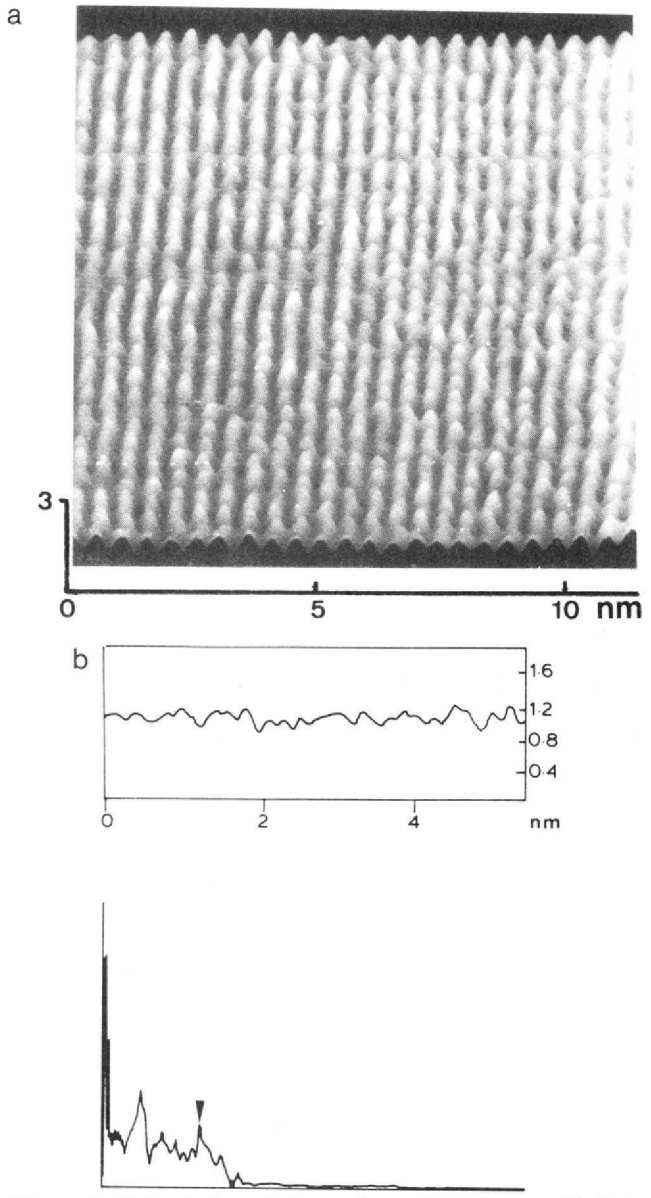

Figure 9. Polyethylene chains at the surface of a nanofibril, $\lambda = 70$: (a) three-dimensional low-pass-filtered representation; (b) surface profile and one-dimensional Fourier transform along the chain. The arrow indicates the 2.5-Å periodicity.

submicron scale. After necking, some microfibrils appear to contain remnants of the original lamellae, while other microfibrils already consist of nanofibrils. This is in agreement with TEM investigations,[20] which showed directly aside blocks which remain rather undeformed, how stacks of folded chain crystals are ripped out of the original arrangement and subsequently converted into fibrils. Microheterogeneity and cooperative deformation of complete stacks of lamellae can also explain the bundling of nanofibrils to microfibrils, i.e., microfibrils.

Once the fibrous structure has been formed, the diameters of the smallest fibrils remain constant while the diameters of the microfibrils and the initially visible bundles of microfibrils are strongly affected by the draw ratio. Consequently, one can conclude that the deformation process is essentially based on two interdependent modes of plastic deformation, i.e., sliding motion of microfibrils and shear deformation of microfibrils due to sliding of the nanofibrils.

In general, the morphology of the drawn tapes is in agreement with data from electron microscopy and X-ray diffraction. In some cases,[12,19] the diameters of "microfibrils" were estimated to be similar in value to those of the nanofibrils in this report, and protofibrils have been discussed as corresponding elementary building units with a rather narrow distribution in diameter.[27,28] It must be noted that the diameter of the nanofibrils as was measured by AFM might be overestimated, depending on the shape of the AFM tip and how densely the fibrils are packed.[26] However, this does not interfere with the observation of the constant diameter of the nanofibrils.

Acknowledgment. The authors are grateful for financial support from DSM, Geleen, The Netherlands.

References and Notes

(1) Northolt, M. G.; Sikkema, D. J. *Adv. Polym. Sci.* **1991**, *8*, 115.
(2) *Liquid Crystalline Polymers*; Weiss, R. A., Ober, C. K., Eds.; ACS Symposium Series 435; American Chemical Society: Washington, DC, 1990.
(3) Smith, P.; Lemstra, P. J. *J. Mater. Sci.* **1980**, *15*, 505.
(4) Kirschbaum, R.; Dingenen, J. L. J. In Intregation of Polymer Science and Technology; Lemstra, P. J., Kleintjens, L. A., Eds.; Elsevier Applied Science: London, 1989; Vol. 2, p 178.
(5) Sawatari, C.; Matsuo, M. *Colloid Polym. Sci.* **1985**, *263*, 783.
(6) Lemstra, P. J.; van Aerle, N. A. J. M.; Bastiaansen, C. W. M. *Polym. J.* **1987**, *19*, 85.
(7) Hoogsteen, W.; Pennings, A. J.; ten Brinke, G. *Colloid Polym. Sci.* **1990**, *268*, 245.
(8) Anandakumaran, K.; Roy, S. K.; Manley, St. J. R. *Macromolecules* **1988**, *21*, 1741, 1746.
(9) Peterlin, A. *J. Mater. Sci.* **1971**, *6*, 490.
(10) van Aerle, N. A. J. M.; Braam, A. W. M. *J. Mater. Sci.* **1988**, *23*, 4429.
(11) van Aerle, N. A. J. M.; Braam, A. W. M. *Colloid Polym. Sci.* **1989**, *267*, 323.
(12) Chanzy, H. D.; Smith, P.; Revol, J.-F.; Manley, St. R. J. *Polym. Commun.* **1987**, *28*, 133.
(13) Binnig, G.; Quate, C. F.; Gerber, Ch. *Phys. Rev. Lett.* **1986**, *56*, 930.
(14) Patil, R.; Kim, S.-J.; Smith, E.; Reneker, D.; Weisenhorn, A. C. *Polym. Commun.* **1990**, *31*, 455.
(15) Reneker, D. H.; Schneir, J.; Howell, B.; Havary, H. *Polym. Commun.* **1990**, *31*, 167.
(16) Magonov, S. N.; Qvarnstrom, K.; Elings, V.; Cantow, H.-J. *Polym. Bull.* **1991**, *25*, 689.
(17) Stocker, W.; Bar, G.; Kunz, M.; Möller, M.; Magonov, S. N.; Cantow, H.-J. *Polym. Bull.* **1991**, *26*, 215.
(18) Magonov, S. N.; Kempf, S.; Kimming, M.: Cantow, H.-J. *Polym. Bull.* **1991**, *26*, 715.
(19) Smith, P.; Lemstra, P. J.; Pijpers, J. P. L.; Kiel, A. M. *Colloid Polym. Sci.* **1981**, *259*, 1070.
(20) Kunz, M.; De Micheli, Möller, M. In *Integration of Fundamental Polymer Science and Technology*; Lemstra, P. J.; Kleintjens, L. A.; Eds.; Elsevier Applied Science: London and New York, 1990; Vol. 4.
(21) Magonov, S. N.; Kempf, S.; Kimmig, M.; Cantow, H.-J. *J. Polym. Sci., Polym. Phys. Ed.* **1991**, *26*, 715.
(22) Grutter, P.; Zimmermann-Edling, W.; Brodbeck, D. *Appl. Phys. Lett.* **1992**, *60*, 2741.
(23) Dijkstra, D. J.; Torfs, J. C. M.; Pennings, A. J. *Colloid Polym. Sei.* **1989**, *267*, 866.
(24) van Aerle, N. A. J. M.; Lemstra, P. J. *Polym. J.* **1988**, *20*, 131.
(25) Sheiko, S. S.; Frey, H.; Möller, M. *Colloid Polym. Sci.* **1992**, *270*, 440.
(26) Vesenka, J.; Guthold, M.; Tang, C. L.; Keller, D.; Delaine, E. *Bustamantel., Ultramicrosc.* **1992**, *42–44*, 1243.
(27) Van Hutten, P. F.; Konig, C. E.; Pennings, A. J. *Makromol. Chem., Rapid. Commun.* **1983**, *4*, 605.
(28) Brady, J. M.; Thomas, E. L. *Polymer* **1989**, *30*, 1615.